Supporting Information

The Importance of Ligand Selection on the Formation of Metal Phosphonate-Derived CoMoP and $CoMoP_2$ Nanoparticles for Catalytic Hydrogen Evolution

Sayed M. El-Refaei, Patrícia A. Russo, Patrick Amsalem, Nobert Koch, and Nicola Pinna**

Sayed M. El-Refaei, Dr. Patrícia A. Russo and Prof. Nicola Pinna
Institut für Chemie and IRIS Adlershof, Humboldt-Universität zu Berlin, Brook-Taylor-Str. 2, 12489 Berlin, Germany.
E-mail: patricia.russo@hu-berlin.de, nicola.pinna@hu-berlin.de

Sayed M. El-Refaei
Chemistry Department, Faculty of Science, Cairo University, Cairo 12613, Egypt.

Dr. Patrick Amsalem, Prof. Nobert Koch
Institut für Physik and IRIS Adlershof, Humboldt-Universität zu Berlin, Brook-Taylor-Str. 6, 12489 Berlin, Germany.

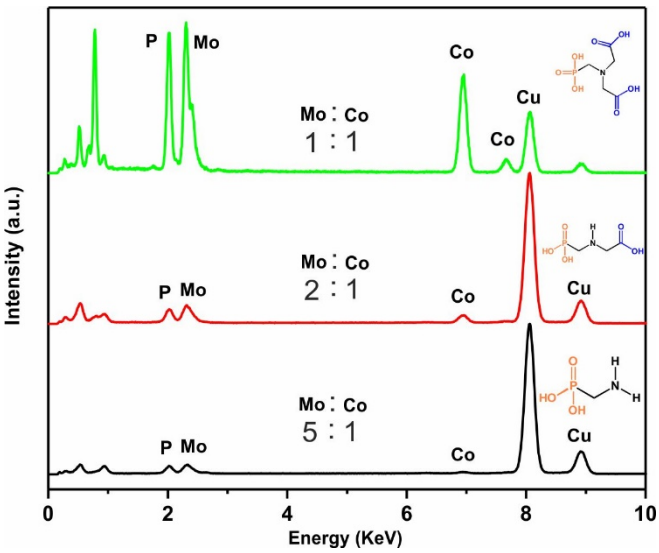

Figure S1. EDS spectra of CPs built from acid 1 (black), 2 (red) and 3 (green).

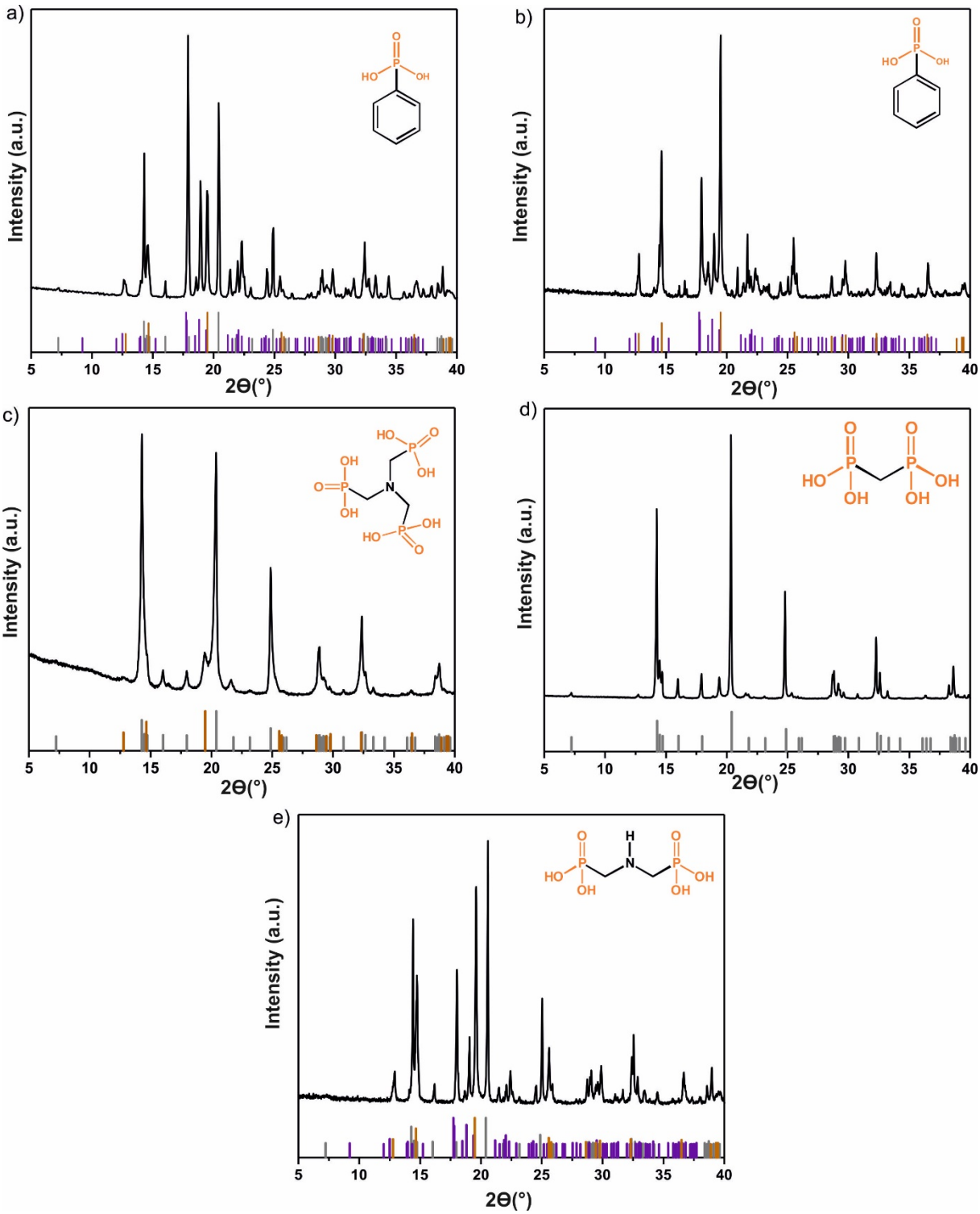

Figure S2. XRD patterns of phosphides derived from CPs based on acids a) 7, b) physical mixture of Mo and Co CPs based on 7, c) 6, d) 5, and e) 4 with doubled molar amount of metals. Vertical bars represent reference patterns: CoMoP violet (ICDD No. 071-0478), brown MoP (ICDD No. 065-6487) and $CoMoP_2$ grey (ICDD No. 033-0428).

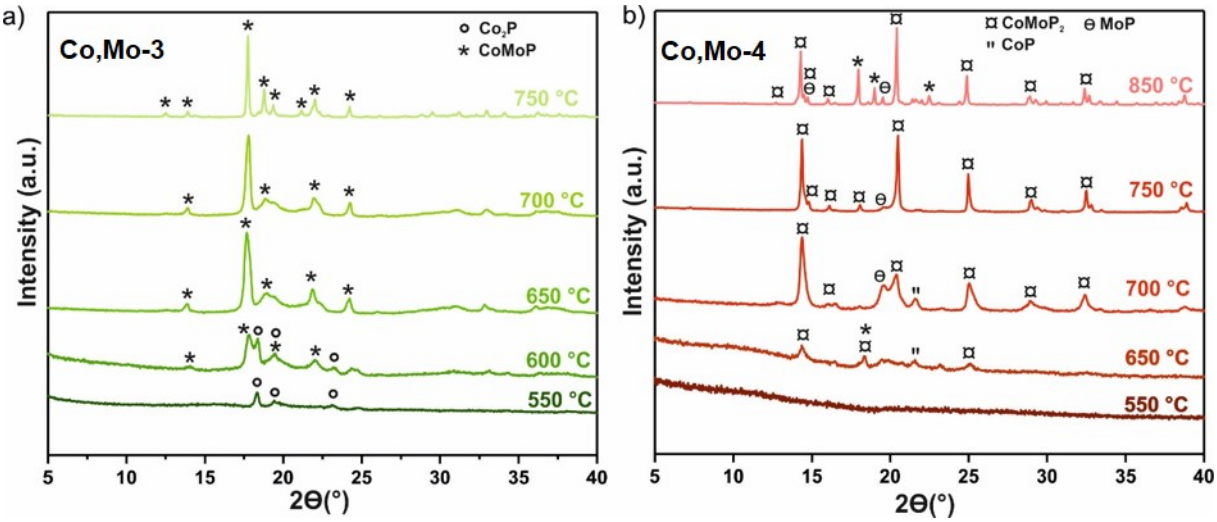

Figure S3. XRD patterns of the products synthesized at different temperatures, from CPs based on acids a) 3 and b) 4.

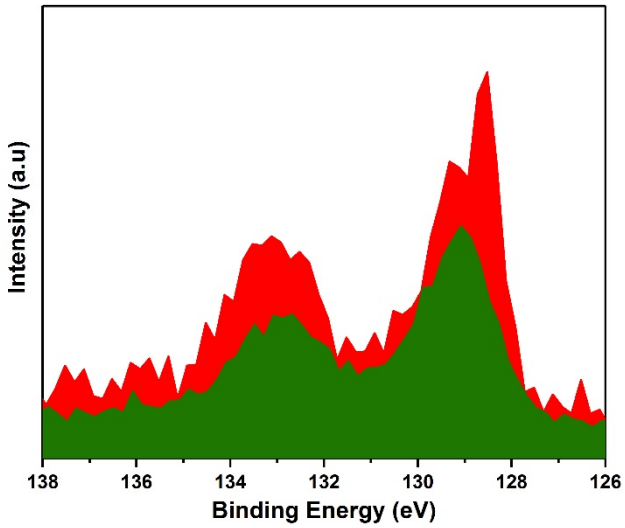

Figure S4. Comparison between the XPS P 2p spectra of the CoMoP (green) and $CoMoP_2$ (red) materials.

Table S1. Stoichiometry of Co, Mo and P at the samples surface, determined by XPS.

Sample	**Co**	**Mo**	**P**
CoMoP	0.9	1	1.1
CoMoP after catalysis	0.6	1.1	1.3
$CoMoP_2$	1	1.2	1.8
$CoMoP_2$ after catalysis	0.5	1.1	2.4

Table S2. Relative percentage of Co, Mo, and P in the phosphide and in oxidized species at the surface of the CoMoP and $CoMoP_2$ nanomaterials, before and after electrocatalysis.

Sample	**$Co_{(phosphide)}$ (%)**	**$Co_{(oxidized)}$ (%)**	**$Mo_{(phosphide)}$ (%)**	**$Mo_{(oxidized)}$ (%)**	**$P_{(phosphide)}$ (%)**	**$P_{(oxidized)}$ (%)**
CoMoP	65	35	42	58	62	38
CoMoP after catalysis	100	0	29	69	65	35
$CoMoP_2$	65	35	60	40	46	54
$CoMoP_2$ after catalysis	100	0	45	55	46	54

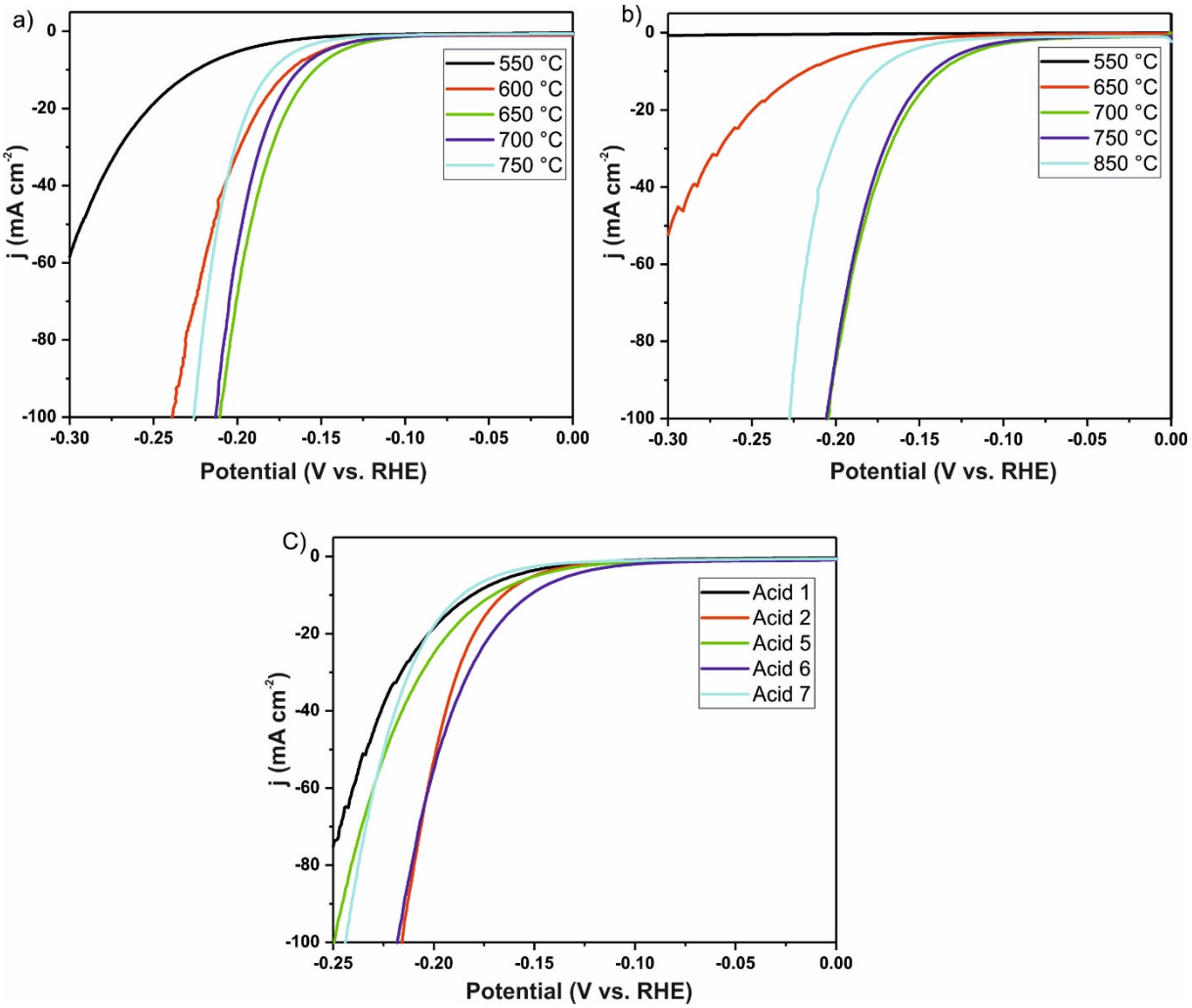

Figure S5. LSVs of the samples derived from a) Co,Mo-3 and b) Co,Mo-4 at different synthesis temperatures; c) LSVs of the samples synthesized at 750 °C, from precursors based on different acid molecules.

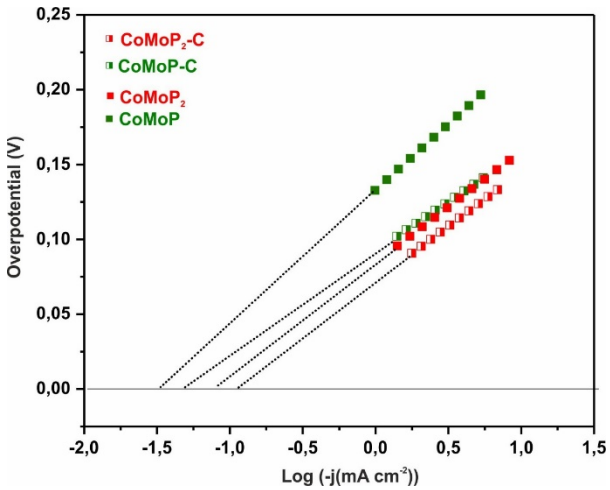

Figure S6. Tafel plots with exchange current density of the CoMoP and $CoMoP_2$ nanomaterials, with and without carbon.

Table S3. Comparison between the electrocatalytic performance of the $CoMoP_x$ HER catalysts studied in this work and literature data (all values reported in 0.5 M H_2SO_4).

Catalyst	**Tafel slope (mV dec^{-1})**	**Overpotential at -10 mA cm^{-2} (mV)**	**Mass loading (µg cm^{-2})**	**TOF s^{-1}**	**Ref.**
MoP@PC	59.3	258	140	------	1
MoP@PC@rGO	53.6	243.6	140	0.019	2
MoP@C@rGO	79	168.9	714	-----	3
CoP/NCNHP	53	140	------	-----	4
Co_2P nanorods	71	134	1000	0.725	5
WP	75	161	500	------	6
MoWP	62	230	215	------	7
CoMoP-2	50	215	66	------	8
CoMoP-0.05	50	215	71	0.28	9
CoMoP-600	136	220	199	-----	10
$CoMoP_2$	60.5	175	400	-----	11
CoMoP@C	49.73	41	354	-----	12
Co-Mo-P@C	52.9	96	1000	-----	13
CoP3/CoMoP/NF	61	125	------	------	14
$NiMoP_2$	56	150	5000	0.15	15
FeMoP-0.1	50	200	71	-----	16
FeP/MoP@NPC	56.6	240	140	-----	17
CoMoP	65.6	150	250	0.4	This work
$CoMoP_2$	72.2	140	250	0.9	This work

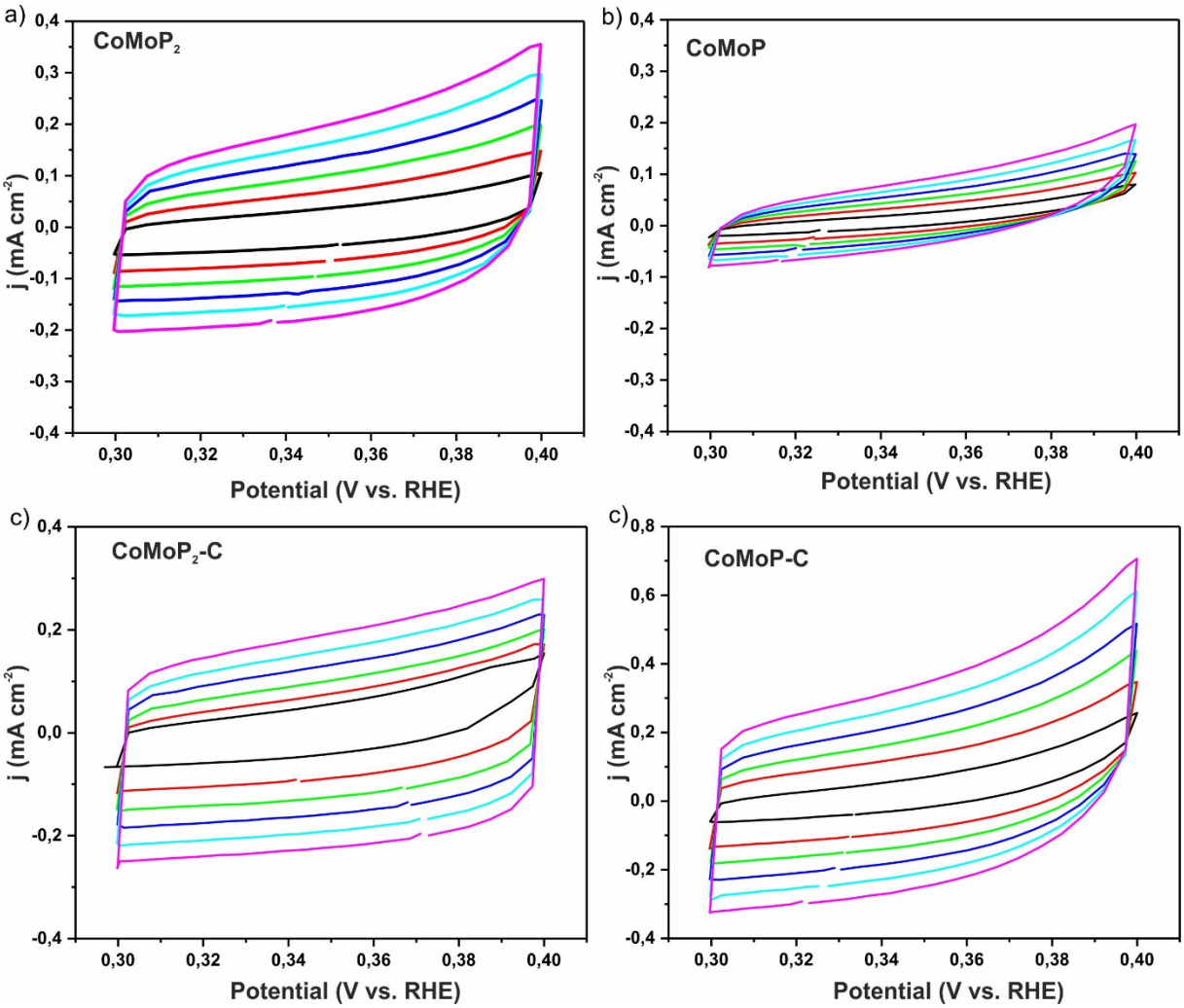

Figure S7. CVs a,c) of $CoMoP_2$ without and with carbon, and b,d) of CoMoP without and with carbon, in the non-Faradaic capacitance current range at scan rates of 10, 20, 30, 40, 50, and 60 mV s^{-1} .

Calculated electrochemical active surface area.

$CoMoP_2$+C:

$$\mathbf{A_{ECSA}^{CoMoP2+C} = \frac{3.17\ mF\ cm^{-2}}{0.04\ \ mF\ cm^{-2}} = 79.25\ cm_{ECSA}^{-2}}$$

$$\mathbf{A_{ECSA}^{CoMoP2} = \frac{2.97\ mF\ cm^{-2}}{0.04\ \ mF\ cm^{-2}} = 74.25\ cm_{ECSA}^{-2}}$$

$$\mathbf{A_{ECSA}^{CoMoP+C} = \frac{4.93\ mF\ cm^{-2}}{0.04\ \ mF\ cm^{-2}} = 123.25\ cm_{ECSA}^{-2}}$$

$$\mathbf{A_{ECSA}^{CoMoP} = \frac{1.015\ mF\ cm^{-2}}{0.04\ \ mF\ cm^{-2}} = 25.375\ cm_{ECSA}^{-2}}$$

Turnover frequency calculations.

To calculate the per-site turnover frequency (TOF), we used the following formula:

$$\mathbf{TOF} = \frac{\mathbf{\#\ total\ hydrogen\ turnovers/\ cm^2\ geometric\ area}}{\mathbf{\#\ active\ sites\ /cm^2\ geometric\ area}}$$

The total number of hydrogen turnovers was calculated from the current density according to:

$$\mathbf{\#H_2} = \left(\mathbf{j}\,\frac{\mathbf{mA}}{\mathbf{cm^2}}\right)\left(\frac{\mathbf{1C\ s^{-1}}}{\mathbf{1000\ mA}}\right)\left(\frac{\mathbf{1\ mol\ e^{-1}}}{\mathbf{96485.3C}}\right)\left(\frac{\mathbf{1\ mol\ H_2}}{\mathbf{2\ mol\ e^{-1}}}\right)\left(\frac{\mathbf{6.022\ x10^{23}\ H_2}}{\mathbf{1\ mol\ H_2}}\right)$$

$$= \mathbf{3.12\ x\ 10^{15}}\,\frac{\mathbf{H_2}}{\mathbf{s.cm^2}}\ \mathbf{Per}\ \frac{\mathbf{mA}}{\mathbf{cm^2}}$$

Since the exact hydrogen binding site numbers is unknown, we estimate the number of active sites as the number of surface sites (including Mo, Co and P atoms as possible active sites) from the roughness factor together with the unit cell (volume = 146.610 and 105.777 $Å^3$ for CoMoP and $CoMoP_2$, respectively, see Figure S7) of both phosphides crystal structure. A similar approach was used to estimate TOF for MoP, MoP/S, Ni_2P and CoP.

active sites per real surface area for $CoMoP_2$:

$$\mathbf{\#\ active\ sites} = \left(\frac{\mathbf{8\ atoms\ /\ unit\ cell}}{\mathbf{105.777\ Å^{\frac{2}{3}}\ /\ unit\ cell}}\right)^{\frac{2}{3}} = \mathbf{1.788\ x\ 10^{15}\ atoms\ cm_{real}^{-2}}$$

active sites per real surface area for CoMoP:

$$\mathbf{\#\ active\ sites} = \left(\frac{\mathbf{12\ atoms\ /\ unit\ cell}}{\mathbf{146.610\ Å^{\frac{2}{3}}\ /\ unit\ cell}}\right)^{\frac{2}{3}} = \mathbf{1.885\ x\ 10^{15}\ atoms\ cm_{real}^{-2}}$$

Therefore, current density can be converted to TOF according to:

$$\mathbf{TOF^{CoMoP2}} = \frac{\left(\mathbf{3.12\ x\ 10^{15}}\,\frac{\mathbf{H_2}}{\mathbf{s.cm^2}}\ \mathbf{Per}\ \frac{\mathbf{mA}}{\mathbf{cm^2}}\right)\mathbf{x\ |j|}}{\left(\mathbf{1.788\ x\ 10^{15}\ atoms\ cm_{real}^{-2}}\right)\mathbf{x\ A_{ECSA}}}$$

and

$$\mathbf{TOF^{CoMoP}} = \frac{\left(\mathbf{3.12\ x\ 10^{15}}\,\frac{\mathbf{H_2}}{\mathbf{s.cm^2}}\ \mathbf{Per}\ \frac{\mathbf{mA}}{\mathbf{cm^2}}\right)\mathbf{x\ |j|}}{\left(\mathbf{1.885\ x\ 10^{15}\ atoms\ cm_{real}^{-2}}\right)\mathbf{x\ A_{ECSA}}}$$

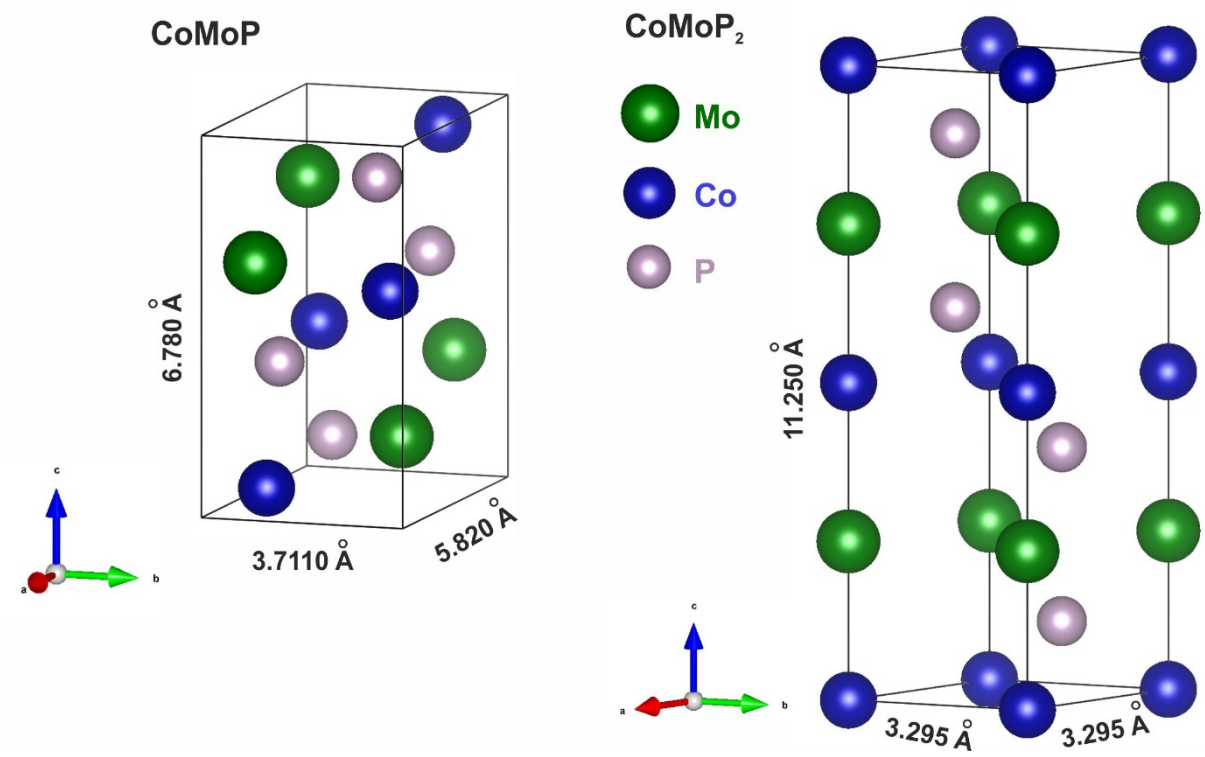

Figure S8. Unit cells representation of CoMoP and $CoMoP_2$.

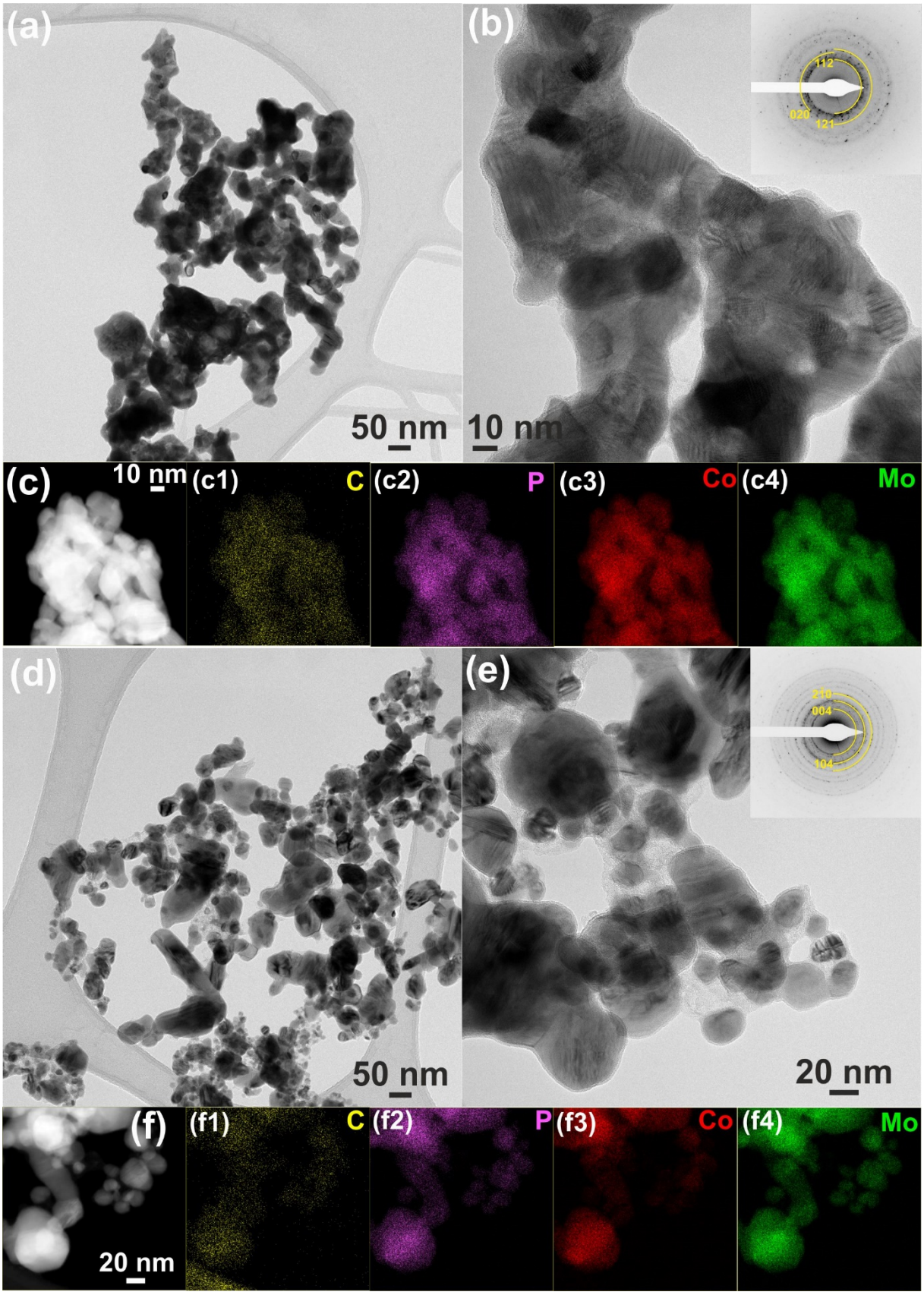

Figure S9. TEM study of the materials after electrocatalysis a,d) TEM and b,e) HRTEM images of CoMoP and $CoMoP_2$; SAED patterns of inset b) CoMoP and e) $CoMoP_2$; HAADF-STEM images of c) CoMoP and f) $CoMoP_2$ and corresponding EDS C, P, Co and Mo elemental maps.

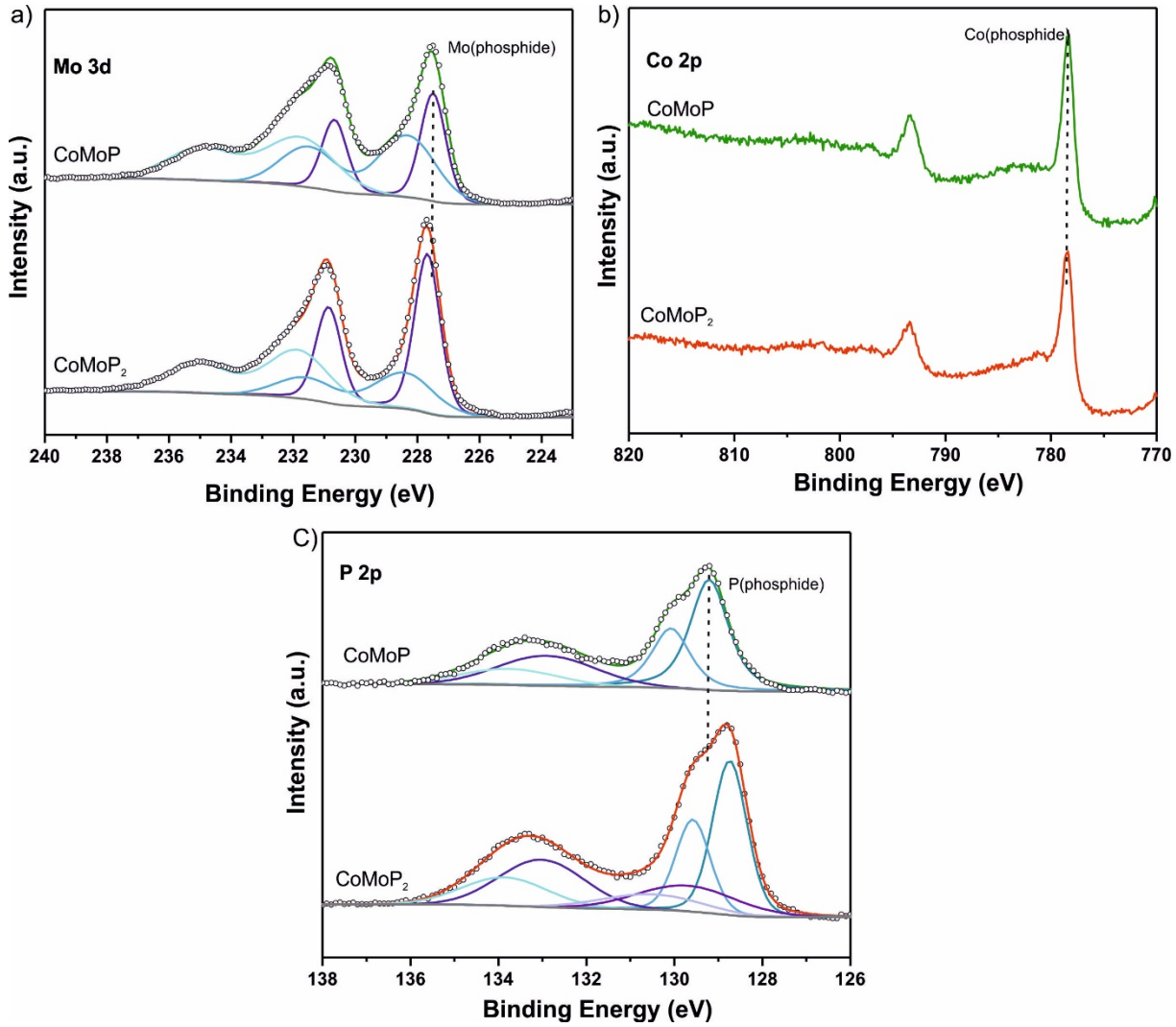

Figure S10. XPS core level of a) Mo 3d, b) Co 2p, and c) P 2p spectra of CoMoP and $CoMoP_2$ after electrocatalysis.

References

1. Li, J.-S.; Zhang, S.; Sha, J.-Q.; Wang, H.; Liu, M.-Z.; Kong, L.-X.; Liu, G.-D., Confined Molybdenum Phosphide in P-Doped Porous Carbon as Efficient Electrocatalysts for Hydrogen Evolution. *ACS Applied Materials & Interfaces* **2018,** 10, (20), 17140-17146.

2. Li, J.-S.; Li, J.-Y.; Wang, X.-R.; Zhang, S.; Sha, J.-Q.; Liu, G.-D., Reduced Graphene Oxide-Supported MoP@P-Doped Porous Carbon Nano-octahedrons as High-Performance Electrocatalysts for Hydrogen Evolution. *ACS Sustainable Chemistry & Engineering* **2018,** 6, (8), 10252-10259.

3. Zhang, Y.; Yang, J.; Dong, Q.; Geng, H.; Zheng, Y.; Liu, Y.; Wang, W.; Li, C. C.; Dong, X., Highly Dispersive MoP Nanoparticles Anchored on Reduced Graphene Oxide Nanosheets for an Efficient Hydrogen Evolution Reaction Electrocatalyst. *ACS Applied Materials & Interfaces* **2018,** 10, (31), 26258-26263.

4. Pan, Y.; Sun, K.; Liu, S.; Cao, X.; Wu, K.; Cheong, W.-C.; Chen, Z.; Wang, Y.; Li, Y.; Liu, Y.; Wang, D.; Peng, Q.; Chen, C.; Li, Y., Core–Shell ZIF-8@ZIF-67-Derived CoP Nanoparticle-Embedded N-Doped Carbon Nanotube Hollow Polyhedron for Efficient Overall Water Splitting. *Journal of the American Chemical Society* **2018,** 140, (7), 2610-2618.

5. Huang, Z.; Chen, Z.; Chen, Z.; Lv, C.; Humphrey, M. G.; Zhang, C., Cobalt Phosphide Panorods as an Efficient Electrocatalyst for the Hydrogen Evolution Reaction. *Nano Energy* **2014,** 9, 373-382.

6. Xing, Z.; Liu, Q.; Asiri, A. M.; Sun, X., High-Efficiency Electrochemical Hydrogen Evolution Catalyzed by Tungsten Phosphide Submicroparticles. *ACS Catalysis* **2015,** 5, (1), 145-149.

7. Yang, L.; Xu, P.; Zhang, W.; Chen, M.; Feng, C.; Yuan, X., Facile Synthesis of One-Dimensional MoWP Hybrid Nanowires and Their Enhanced Electrochemical Catalytic Activities. *Chemical Physics Letters* **2020,** 741, 137107.

8. Wang, D.; Zhang, X.; Zhang, D.; Shen, Y.; Wu, Z., Influence of Mo/P Ratio on CoMoP Nanoparticles as Highly Efficient HER Catalysts. *Applied Catalysis A: General* **2016,** 511, 11-15.

9. Wang, D.; Zhang, D.; Tang, C.; Zhou, P.; Wu, Z.; Fang, B., Hydrogen Evolution Catalyzed by Cobalt-Promoted Molybdenum Phosphide Nanoparticles. *Catalysis Science & Technology* **2016,** 6, (6), 1952-1956.

10. Lin, Y.; Liu, M.; Pan, Y.; Zhang, J., Porous Co–Mo Phosphide Nanotubes: An Efficient Electrocatalyst for Hydrogen Evolution. *Journal of Materials Science* **2017,** 52, (17), 10406-10417.

11. Fang, S.-L.; Chou, T.-C.; Samireddi, S.; Chen, K.-H.; Chen, L.-C.; Chen, W.-F., Enhanced Hydrogen Evolution Reaction on Hybrids of Cobalt Phosphide and Molybdenum Phosphide. *Royal Society Open Science* **2017,** 4, (3), 161016.

12. Ma, Y.-Y.; Wu, C.-X.; Feng, X.-J.; Tan, H.-Q.; Yan, L.-K.; Liu, Y.; Kang, Z.-H.; Wang, E.-B.; Li, Y.-G., Highly Efficient Hydrogen Evolution from Seawater by a Low-cost and Stable CoMoP@C Electrocatalyst Superior to Pt/C. *Energy & Environmental Science* **2017,** 10, (3), 788-798.

13. Gong, L.; Lan, K.; Wang, X.; Huang, X.; Jiang, P.; Wang, K.; Yang, M.; Ma, L.; Li, R., Carbon-Coated Co-Mo-P Nanosheets Supported on Carbon Cloth as Efficient Electrocatalyst for Hydrogen Evolution Reaction. *International Journal of Hydrogen Energy* **2020,** 45, (1), 544-552.

14. Jiang, D.; Xu, Y.; Yang, R.; Li, D.; Meng, S.; Chen, M., CoP3/CoMoP Heterogeneous Nanosheet Arrays as Robust Electrocatalyst for pH-Universal Hydrogen Evolution Reaction. *ACS Sustainable Chemistry & Engineering* **2019,** 7, (10), 9309-9317.

15. Wang, X.-D.; Chen, H.-Y.; Xu, Y.-F.; Liao, J.-F.; Chen, B.-X.; Rao, H.-S.; Kuang, D.-B.; Su, C.-Y., Self-supported NiMoP2 Nanowires on Carbon Cloth as an Efficient and Durable Electrocatalyst for Overall Water Splitting. *Journal of Materials Chemistry A* **2017,** 5, (15), 7191-7199.

16. Liang, X.; Zhang, D.; Wu, Z.; Wang, D., The Fe-Promoted MoP Catalyst with High Activity for Water Splitting. *Applied Catalysis A: General* **2016,** 524, 134-138.

17. Li, J.-S.; Zhang, S.; Sha, J.-Q.; Li, J.-Y.; Wang, X.-R.; Wang, H., A Polyoxometalate-Based Metal–Organic Framework-Derived FeP/MoP Hybrid Encapsulated in N/P Dual-Doped Carbon as Efficient Electrocatalyst for Hydrogen Evolution. *Crystal Growth & Design* **2018,** 18, (8), 4265-4269.